


SPRING-8/SACLA Research Frontiers 2021

CONTENTS

Preface	5
Editor's Note	6
Scientific Frontiers	7
Reviews	
Iron and Hydrogen – Characterization of Fe-H Bonding in Hydrogenases and Model Compounds Using Nuclear Resonant Vibrational Spectroscopy (NRVS) <i>H. Wang and S. P. Cramer</i>	8
Hydrogen and Other Light Elements in the Earth's Core <i>K. Hirose and S. Tagawa</i>	12
Life Science	
Protein Crystallography: Structural insights into allosteric modulation of mGlu2 <i>S. Lin, J. Du, B. Wu and Q. Zhao</i>	16
Protein Crystallography: A small compound 5h blocks the infectivity, replication, and cytopathicity of SARS-CoV-2 via inhibition of main protease <i>K. Hattori and H. Mitsuya</i>	18
Protein Crystallography: Crystal structure of engineered ACE2 complexed with SARS-CoV-2 Spike RBD <i>T. Arimori and J. Takagi</i>	20
Protein Crystallography: Structural basis for FXIIa inhibition by a peptide foldamer containing cyclic β -amino acids <i>T. Sengoku</i>	22
Protein Crystallography: Structural basis of the extracellular interaction between receptor-type tyrosine-protein phosphatase δ and neuroligin 3 <i>S. Fukai</i>	24
Protein Crystallography: Structural basis of heme-responsive sensor protein mediating the survival of hemolytic bacteria <i>H. Sawai and Y. Shiro</i>	26
Protein Crystallography: Molecular basis for two stereoselective Diels–Alderase that form enantiomeric decalin skeletons <i>N. Kato and S. Nagano</i>	28
 Femtosecond Crystallography: Characterization of short-lived reaction intermediate in enzymatic nitrous oxide generation by XFEL crystallography and time-resolved spectroscopy <i>T. Tozha, M. Kubo and Y. Shiro</i>	30
Diffraction X-ray Tracking: Direct observation of capsaicin-induced intramolecular dynamics of TRPV1 channel <i>K. Mio, S. Fujimura and Y. C. Sasaki</i>	32
Otology: 3D imaging of auditory osteoblasts using a Talbot phase-sensitive X-ray tomographic microscope <i>Y. Kuroda</i>	34
Lipids in Cricket: In search of real images of insect cuticular lipids: Synchrotron radiation FTIR ATR microspectroscopy study on insect body surfaces <i>F. Kaneko and C. Katagiri</i>	36

Physical Science

Ceramics Synthesis Process: Observation and modeling of multicomponent ceramics synthesis: A case study of $\text{YBa}_2\text{Cu}_3\text{O}_{6+x}$ <i>A. Miura, C. J. Bartel and W. Sun</i>	38
Semiconductor Device Physics: <i>In situ</i> time-resolved synchrotron radiation nanobeam X-ray diffraction analysis of inverse-piezoelectric-effect-induced lattice deformation in AlGaIn/GaN high-electron-mobility transistors <i>T. Tohei, Y. Imai and A. Sakai</i>	40
Supercritical Water: Liquid-like and gas-like dynamics in supercritical fluids <i>P. Sun, J. B. Hastings and G. Monaco</i>	42
Lipid Dynamics: Molecular origins of two-dimensional membrane viscosity measured by X-ray and neutron spectroscopies <i>M. Nagao</i>	44
Nano-confined Liquid: Structural characterization of nano-confined liquids by synchrotron X-ray diffraction measurement <i>M. Mizukami</i>	46
Invar Alloy: Elongation of Fe–Fe atomic pairs in $\text{Fe}_{65}\text{Ni}_{35}$ Invar alloy determined by RMC method <i>N. Ishimatsu and N. Kitamura</i>	48
Li-ion Battery: Tomographic reconstruction of “orphaned” oxygen orbitals in Li-rich battery material $\text{Li}_x\text{Ti}_{0.4}\text{Mn}_{0.4}\text{O}_2$ <i>K. Suzuki and H. Hafiz</i>	50
RIXS for Heusler Alloys: Probing spin-polarized electronic structures of half-metallic Heusler alloys using resonant inelastic soft X-ray scattering in a magnetic field <i>H. Fujiwara and R. Y. Umetsu</i>	52
Spin-resolved HAXPES: Probing spin-resolved valence band electronic structures of buried Fe film with hard X-ray photoemission <i>S. Ueda</i>	54
Coherent Diffraction Imaging: Dynamic nanoimaging of extended objects via hard X-ray multiple-shot coherent diffraction with projection illumination optics <i>Y. Takayama and Y. Kagoshima</i>	56
Magnetic Octupole Order: Observation of magnetic octupole order producing anomalous Hall effect by X-ray magnetic circular dichroism <i>M. Kimata, N. Sasabe and T. Nakamura</i>	58
Magnetic Friedel Oscillation: Magnetic Friedel oscillation at Fe(001) surfaces: Direct observation by atomic-layer-resolved synchrotron radiation ^{57}Fe Mössbauer spectroscopy <i>T. Mitsui</i>	60
GaN Wafer Topography: Local lattice-plane orientation mapping of 6-inch GaN wafer using X-ray diffraction topography <i>O. Sakata and J. Kim</i>	62
 Astrophysics: Diagnosing plasma turbulence down to the micrometer scale <i>G. Rigon and B. Albertazzi</i>	64
 Split-pulse XPCS: X-ray laser illuminates the local motion of water molecules <i>Y. Shinohara, T. Osaka and I. Inoue</i>	66

Chemical Science

Operando HAXPES: Simultaneous analytical system of electrochemical reaction rate and <i>operando</i> hard X-ray photoemission spectroscopy <i>J. Inukai</i>	68
---	----

Operando AP-HAXPES: Sulfur poisoning Pt and PtCo anode catalysts in polymer electrolyte fuel cells studied by <i>operando</i> near ambient pressure hard X-ray photoelectron spectroscopy <i>T. Yokoyama</i>	70
Operando AP-HAXPES: Quick <i>operando</i> ambient-pressure hard X-ray photoelectron spectroscopy for reaction kinetic measurements of polymer electrolyte fuel cells <i>T. Yokoyama</i>	72
Transition-metal Perovskite Oxide: Spin reorientation of Fe ³⁺ induced by peculiar Pb charge ordering in PbFeO ₃ <i>M. Azuma, Y. Long and T. Nishikubo</i>	74
Li-ion Battery: Structural characterization of the delithiated noncrystalline phase in a Li-rich Li ₂ VO ₂ F cathode material <i>S. Hiroi, K. Ohara and O. Sakata</i>	76
MOF Heterostructure: Control of spin transition by interface strain in heterostructured metal-organic framework thin film <i>T. Haraguchi</i>	78
Operando Spectromicroscopy: Molecular crystalline capsules that release their contents upon irradiation <i>K. Uchida, A. Nagai and R. Nishimura</i>	80
Operando Spectroscopy: Impact of <i>operando</i> X-ray spectromicroscopy for constructing Beyond 5G toward the realization of Society 5.0 <i>H. Fukidome</i>	82
Polymer Hierarchical Structure: Effect of submicron structures on the mechanical behavior of polyethylene <i>M. Takenaka</i>	84
High Resolution XANES: High-sensitivity analysis of fluorescence XANES at Eu L _{III} -edge for the determination of oxidation state for trace amount of Eu in natural samples using Bragg-type crystal analyzer system <i>Y. Takahashi and R. Konagaya</i>	86
Radiocesium-bearing Microparticle: Widespread distribution of radiocesium-bearing microparticles from the Fukushima nuclear accident <i>Y. Abe</i>	88
Environmental Mercury Removal: Identification of chemical species of iodine and mercury on iodine-impregnated activated carbon using X-ray absorption near-edge structure analysis <i>Y. Cheng, K. Shiota and M. Takaoka</i>	90
TES Detector: Broad-band high-energy-resolution hard X-ray spectroscopy using transition edge sensors (TESs) and its application to environmental samples <i>S. Yamada and Y. Takahashi</i>	92

Earth & Planetary Science



Dynamic Compression: Ultrafast structure transformation of olivine to ringwoodite during laser-driven shock compression <i>T. Okuchi</i>	94
Mantles' Discontinuity: Akimotoite-bridgmanite phase transition explains depressed 660-km seismic discontinuity in subduction zones <i>A. Chanyshiev, T. Ishii and T. Katsura</i>	96
Earth's Mantle Chemistry: Crystal chemistry of bridgmanite in a subducting mid-ocean ridge basalt: incorporation mechanism of Fe and Al <i>A. Nakatsuka</i>	98
Planetary Formation: CO ₂ -bearing fluid discovered in a meteorite: evidence of dynamic evolution of the solar system <i>A. Tsuchiyama</i>	100

Industrial Applications

- Li-ion Battery:** Investigation of reaction mechanism of crystalline aromatic dicarboxylate in Li⁺ intercalation by hard X-ray photoelectron spectroscopy 102
R. Mikita and N. Ogihara
- Skin Care Products:** Moisturizing mechanism of glycerol and diglycerol on human stratum corneum 104
A. Habuka, T. Yamada and I. Hatta

Accelerators & Beamlines Frontiers 106

SPRING-8

- Beam Performance** - Recent update on accelerators 107
- New Apparatus, Upgrades & Methodology**
- Hard X-ray nanobeam scanning using advanced Kirkpatrick-Baez mirrors and prisms 108
J. Yamada and M. Yabashi
 - Guidelines for high-efficiency/accuracy data collection with multiple small-wedge data collection using the automatic data collection ZOO system 110
S. Baba

SACLA

- Beam Performance** 113

Facility Status 114

- SPRING-8 Facility Status** 115
- Introduction 115
 - Machine Operation 116
 - Beamlines 117
 - User Program and Statistics 120
 - Research Outcome 123
 - Budget and Personnel 123
 - Research Complex 123
 - SPRING-8 Users Community (SPRUC) 126
 - Outreach Activities 127
- SACLA Facility Status** 128

Note: The principal publication(s) concerning each article is indicated with all author's names in italics in the list of references.